A New Perspective on Coupling Numerator Models

Frederik A. Döring
German Aerospace Center (DLR)
Institute of Flight Systems
Braunschweig, Germany

ABSTRACT

Coupling numerator models are a well-established tool for predicting the closed-loop dynamics of multiple-input multiple-output systems. They describe the input-output dynamics of the open-loop path in a partially controlled system given tight controls and thus may serve as an approximation of the actual dynamics "seen" by the single-axis controller in a controlled multiple-input multiple-output plant. Such models can therefore be employed for a decentralized initial design of multivariable controllers. This paper presents a new, unifying approach for the computation of such constrained input-output dynamics. Connections to existing methods in the literature are established and a general procedure for state-space calculations is given. The use of coupling numerator models for controller design is motivated and different decoupling structures are discussed. The controller design is illustrated using a coupled high-order helicopter model.

NOTATION

List of Symbols

A	system matrix
B, B_1, B_2	input matrices
C, C_1, C_2	output matrices
d	derivative order
$D, D_{11}, D_{12}, D_{21}, D_{22}$	feedthrough matrices
f_1, f_2	feedforward signals
i, j, k, l	integer indices
K_{11}, K_{22}	feedback controllers
K_{21}, K_{12}	decoupling controller crossfeeds
$L(s), M(s)$	derivative filter
n_2	dimension of y_2
P	plant model
$P_{11}, P_{12}, P_{21}, P_{22}$	plant subsystems
$Q_{11}, Q_{12}, Q_{21}, Q_{22}$	coupling numerator models for channel 1
r_1, r_2	reference signals
$r_{l,i}$	relative degree from u_l to $y_{2,i}$
r_l^{vec}	vector relative degree
$R_{11}, R_{12}, R_{21}, R_{22}$	coupling numerator models for channel 2
s	Laplace variable
S, S_1, S_2	transformation matrices
T, T_1, T_2	inverse transformation matrices
u_1, u_2	input signals
x	state variable
y_1, y_2	output signals
η	state of inverse system
ξ	auxiliary output variable

List of Acronyms

ACT/FHS	Active Control Technology/ Flying Helicopter Simulator
MIMO	multiple-input multiple-output
PID	proportional–integral–derivative
SISO	single-input single-output

INTRODUCTION

The design of feedback controllers for multiple-input multiple-output (MIMO) systems is a challenging task. This is especially true for systems which exhibit non-negligible cross-couplings such as helicopters. In practice, simple, sequential, decentralized controller designs ("one loop at a time") are usually preferred over (unstructured) full-order approaches as they offer more transparency during the design process and allow for easier interpretation and tuning of the involved controller parameters (Ref. 1). While such a controller design only based on the open loop dynamic behavior might be still viable for weakly coupled systems, the plant-controller couplings must be explicitly taken into account to obtain a good closed-loop performance for strongly coupled systems. Coupling numerator models are a way to account for such plant-controller interactions during sequential controller design (Ref. 1).

Coupling numerators are inferred from calculating the input-output dynamics of a partially controlled system based on Cramer's Rule for solving linear equations and were originally formulated in the frequency domain (Ref. 2). A a state-space procedure for calculating coupling numerator models was first presented in (Ref. 3). Coupling numerators can be used to design crossfeeds (Ref. 4) and study the effects of different input-output pairings (Ref. 5) on the closed-loop dynamics. The effect of pilot dynamics on the aeromechanic stability of

Presented at the Vertical Flight Society's 80th Annual Forum & Technology Display, Montréal, Québec, Canada, May 7–9, 2024.

low-frequency rotor modes by using coupling numerator models was investigated in (Ref. 6). However, calculating coupling numerators can become tedious for large systems with many control channels, an aspect that was already addressed in (Ref. 6) and also later in (Ref. 3). Although introduced six decades ago, coupling numerators are still considered to be a valuable tool for system analysis and preliminary controller design (Ref. 1).

The established methods for calculating coupling numerator models have some drawbacks, however. Although being capable of taking model output equations into account, the frequency domain based approach (Ref. 2) only yields single-input single-output (SISO) models which might be unsuitable for some applications. On the other hand, the state-space method from (Ref. 3), while being capable of creating constrained MIMO models, can only handle state but not output equations. In contrast, the approach presented in this paper achieves both. It can handle linear system equations in great generality and yields constrained plant dynamics of arbitrary size.

This paper is structured as follows: The first section presents a new approach to the computation of constrained input-output models and the involved crossfeeds and discusses how these results relate to previous approaches. The second section provides a general procedure for computing state-space realizations followed by a brief third section on the dynamic properties of coupling numerator models. The fourth section motivates how these models can be employed in multivariable controller design and studies the effect of introducing crossfeeds to the design. The last section illustrates the controller design procedure for a real-world coupled high-order helicopter model in hover.

AN ALTERNATIVE DERIVATION OF COUPLING NUMERATOR MODELS

The new approach assumes that a dynamic system P is given that describes the input-output behavior of a MIMO system (e.g. a transfer function matrix or a state-space model). Let the inputs $u^T = \begin{pmatrix} u_1^T & u_2^T \end{pmatrix}$ and the outputs $y^T = \begin{pmatrix} y_1^T & y_2^T \end{pmatrix}$ be separated into two channels with the system P partitioned accordingly, i.e.

$$\begin{pmatrix} y_1 \\ y_2 \end{pmatrix} = \begin{pmatrix} P_{11} & P_{12} \\ P_{21} & P_{22} \end{pmatrix} \begin{pmatrix} u_1 \\ u_2 \end{pmatrix} \tag{1}$$

or, equivalently,

$$\begin{aligned} y_1 &= P_{11}u_1 + P_{12}u_2 \\ y_2 &= P_{21}u_1 + P_{22}u_2 \end{aligned} \tag{2}$$

Channel 1 can be of arbitrary size, P_{22} is assumed to be square and invertible. The goal is to derive a model for the input-output behavior of channel 1 under the assumption that the feedback loop of channel 2 is "tightly" closed. Let K_{22} denote the (constant) feedback gain of channel 2 and r_2 denote the reference for the controlled output y_2. It is assumed that K_{22} is invertible. Fig. 1 depicts the setup. Since

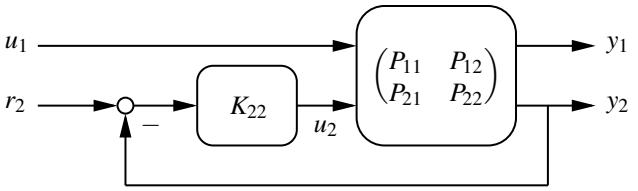

Figure 1: A partially closed-loop system

$$u_2 = K_{22}(r_2 - y_2) \tag{3}$$

one can solve the second equation in (2) for y_2 which leads to

$$y_2 = (I + P_{22}K_{22})^{-1}P_{21}u_1 + (I + P_{22}K_{22})^{-1}P_{22}K_{22}r_2 \tag{4}$$

Plugging this expression into eq. (3) yields

$$u_2 = -K_{22}(I + P_{22}K_{22})^{-1}P_{21}u_1 + K_{22}(I + P_{22}K_{22})^{-1}r_2 \tag{5}$$

which together with the first equation in (2) leads to

$$\begin{aligned} y_1 = &\left(P_{11} - P_{12}K_{22}(I + P_{22}K_{22})^{-1}P_{21}\right)u_1 \\ &+ P_{12}K_{22}(I + P_{22}K_{22})^{-1}r_2 \end{aligned} \tag{6}$$

Since K_{22} is invertible, it holds that

$$\begin{aligned} K_{22}(I + P_{22}K_{22})^{-1} &= K_{22}\left((K_{22}^{-1} + P_{22})K_{22}\right)^{-1} \\ &= (K_{22}^{-1} + P_{22})^{-1} \end{aligned} \tag{7}$$

Therefore, when letting $K_{22} \to \infty$ (tightening the loop-closure of channel 2), one obtains from eqs. (5) and (6)

$$\begin{aligned} y_1 &= \left(P_{11} - P_{12}P_{22}^{-1}P_{21}\right)u_1 + P_{12}P_{22}^{-1}r_2 \\ u_2 &= -P_{22}^{-1}P_{21}u_1 + P_{22}^{-1}r_2 \end{aligned} \tag{8}$$

Increasing K_{22} acts as high-gain feedback for channel 2 effectively inverting its input-output behavior and forcing y_2 to converge to r_2. Thus, one could have also arrived at these expressions by starting from eq. (1) and just inverting the relation between y_2 and u_2 and replacing y_2 with r_2 afterwards yielding

$$\begin{aligned} \begin{pmatrix} y_1 \\ u_2 \end{pmatrix} &= \begin{pmatrix} P_{11} - P_{12}P_{22}^{-1}P_{21} & P_{12}P_{22}^{-1} \\ -P_{22}^{-1}P_{21} & P_{22}^{-1} \end{pmatrix} \begin{pmatrix} u_1 \\ r_2 \end{pmatrix} \\ &=: \begin{pmatrix} Q_{11} & Q_{12} \\ Q_{21} & Q_{22} \end{pmatrix} \begin{pmatrix} u_1 \\ r_2 \end{pmatrix} \end{aligned} \tag{9}$$

The element Q_{11} is the desired open-loop dynamics from u_1 to y_1 given that channel 2 is tightly controlled. If either of the off-diagonal plant components of the original plant (P_{12} or P_{21}) is small, control channel 1 will not be affected much by the loop closure of channel 2 meaning both channels are rather decoupled. The Q_{12}-element describes the impact of the reference r_2 on the uncontrolled output y_1. In cases where the reference r_2 is known (measurable), disturbance feedforward compensation strategies can be employed to counteract its influence on y_1. The Q_{21}-element reflects how much u_1 affects the controls of channel 2. It can be used to design feedback

decoupling crossfeeds.
Note that the subsystem P_{11} is not required to be square. For example, y_1 could contain several output variables of interest, even those not directly affected by u_1. The input u_1 could contain also independent exogenous input variables (like disturbance inputs) or could even be empty (in which case y_1 only depends on r_2).

Relation to Other Approaches

Originally, coupling numerator models were derived from Laplace-transformed, linearized equations of motion using Cramer's rule for solving linear equations. The considerations in McRuer et al. (Ref. 2) begin with stating the transformed equations of motion

$$\begin{pmatrix} a_{11} & a_{12} \\ a_{21} & a_{22} \end{pmatrix} \begin{pmatrix} y_1 \\ y_2 \end{pmatrix} = \begin{pmatrix} b_{11} & b_{12} \\ b_{21} & b_{22} \end{pmatrix} \begin{pmatrix} u_1 \\ u_2 \end{pmatrix} \tag{10}$$

where the matrix coefficients are, in general, functions of the Laplace variable s and it is assumed that channel 1 is SISO and channel 2 is square. By applying Cramer's rule, it is possible to explicitly derive expressions for the numerator and denominator of the transfer function of a given input-output pair. When these transfer functions are constrained by feedback, their numerators and denominators consist of special determinants which are called *coupling numerators*. However, for large systems this can lead to cumbersome expressions that may be hard to interpret.
Recall that according to Schur's formula the determinant of a partitioned matrix M with invertible subcomponent M_{22} is calculated as

$$\begin{aligned} \det(M) &= \det \begin{pmatrix} M_{11} & M_{12} \\ M_{21} & M_{22} \end{pmatrix} \\ &= \det(M_{22}) \det(M_{11} - M_{12} M_{22}^{-1} M_{21}) \end{aligned} \tag{11}$$

The derivations in (Ref. 2) are valid for arbitrary transfer function matrix coefficients. In order to establish equivalence with the approach presented above, it is hence valid to use eq. (1) instead of eq. (10) (the former is a special case of the latter). Then insert the feedback law (3) to obtain

$$\begin{pmatrix} 1 & P_{12}K_{22} \\ 0 & (I + P_{22}K_{22}) \end{pmatrix} \begin{pmatrix} y_1 \\ y_2 \end{pmatrix} = \begin{pmatrix} P_{11} & P_{12}K_{22} \\ P_{21} & P_{22}K_{22} \end{pmatrix} \begin{pmatrix} u_1 \\ r_2 \end{pmatrix} \tag{12}$$

Now apply Cramer's rule to extract the dependence of y_1 on u_1 from this equation resulting in

$$\begin{aligned} \left.\frac{y_1}{u_1}\right|_{u_2 \to y_2} &= \det \begin{pmatrix} P_{11} & P_{12}K_{22} \\ P_{21} & (I + P_{22}K_{22}) \end{pmatrix} \det(I + P_{22}K_{22})^{-1} \\ &= \det(P_{11} - P_{12}K_{22}(I + P_{22}K_{22})^{-1} P_{21}) \end{aligned} \tag{13}$$

where Schur's formula is applied at the second equality sign. The notation $y_1/u_1|_{u_2 \to y_2}$ used here intends to characterize the transfer function from u_1 to y_1 given that there is a feedback from y_2 to u_2. Letting $K_{22} \to \infty$ as in the previous section yields

$$\left.\frac{y_1}{u_1}\right|_{u_2 \to y_2} = \det(P_{11} - P_{12}P_{22}^{-1}P_{21}) = P_{11} - P_{12}P_{22}^{-1}P_{21} \tag{14}$$

which is equivalent to the expression for Q_{11} in eq. (9). Later, Hess (Ref. 5) derived an alternative representation assuming channel 2 is SISO as well

$$\left.\frac{y_1}{u_1}\right|_{u_2 \to y_2} = \frac{\det(P)}{P_{22}} \tag{15}$$

which can be recognized as a special case of Schur's formula applied to P

$$\det(Q_{11}) = \det(P)\det(P_{22}^{-1}) \tag{16}$$

The Q_{21} element relates to plant input decoupling and eliminates the impact of u_1 on y_2

$$\begin{pmatrix} P_{11} & P_{12} \\ P_{21} & P_{22} \end{pmatrix} \begin{pmatrix} I & 0 \\ Q_{21} & I \end{pmatrix} = \begin{pmatrix} P_{11} - P_{12}P_{22}^{-1}P_{21} & P_{12} \\ 0 & P_{22} \end{pmatrix} \tag{17}$$

The resulting dynamics for channel 1 are given by Q_{11}. Note that this simplifies the calculation of crossfeeds for single control axes compared to how it is done in (Ref. 4) as the crossfeed follows immediately from eq. (9).
The Q_{12} element relates relates to plant output decoupling and eliminates the influence of u_2 on y_1

$$\begin{pmatrix} I & -Q_{12} \\ 0 & I \end{pmatrix} \begin{pmatrix} P_{11} & P_{12} \\ P_{21} & P_{22} \end{pmatrix} = \begin{pmatrix} P_{11} - P_{12}P_{22}^{-1}P_{21} & 0 \\ P_{21} & P_{22} \end{pmatrix} \tag{18}$$

Using the established notation in the literature one may write

$$\begin{pmatrix} Q_{11} & Q_{12} \\ Q_{21} & Q_{22} \end{pmatrix} = \begin{pmatrix} \left.\frac{y_1}{u_1}\right|_{u_2 \to y_2} & \left.\frac{y_1}{r_2}\right|_{u_2 \to y_2} \\ \left.\frac{u_2}{u_1}\right|_{u_2 \to y_2} & \left.\frac{u_2}{r_2}\right|_{u_2 \to y_2} \end{pmatrix} \tag{19}$$

Example

Consider the following system

$$P = \left(\begin{array}{c|cc} P_{11} & P_{12} \\ \hline P_{21} & P_{22} \end{array}\right) = \left(\begin{array}{cc|cc} \frac{2}{(s+1)^2} & & 0 & \frac{1}{s+2} \\ & & 2 & 0 \\ \frac{1}{s+5} & & \frac{2(s+1)}{s+2} & \frac{2}{s+2} \\ 0 & & & \end{array}\right) \tag{20}$$

The inverse of P_{22} is given by

$$Q_{22} = \frac{1}{2}\begin{pmatrix} 1 & 0 \\ -(s+1) & s+2 \end{pmatrix} \tag{21}$$

and it follows that

$$Q_{11} = \frac{2}{(s+1)^2} + \frac{s+1}{2(s+2)(s+5)} \tag{22}$$

$$Q_{12} = \frac{1}{2}\begin{pmatrix} -\frac{s+1}{s+2} & 2 \end{pmatrix} \tag{23}$$

and

$$Q_{21}^T = \frac{1}{2}\begin{pmatrix} -\frac{1}{s+5} & \frac{s+1}{s+5} \end{pmatrix} \tag{24}$$

A GENERAL STATE-SPACE PROCEDURE

In practice, state-space realizations are are easier to work with than transfer functions and lead to more compact realizations, especially for MIMO models. Consider a state-space realization of eq. (2) given by

$$\begin{aligned} \dot{x} &= Ax + B_1 u_1 + B_2 u_2 \\ y_1 &= C_1 x + D_{11} u_1 + D_{12} u_2 \\ y_2 &= C_2 x + D_{21} u_1 + D_{22} u_2 \end{aligned} \tag{25}$$

where, as above, an expression describing the u_1/y_1 dynamics given tight control of channel 2 is to be derived. As can be seen from eq. (9), the coupling numerator models are based on a partial inversion of the system equations. For system inversion in state space, one can distinguish two cases.

The Trivial Case: D_{22} Non-singular

In this case, one can directly solve eq. (25) for u_2 and obtains

$$\begin{aligned} \dot{\eta} &= (A - B_2 D_{22}^{-1} C_2)\eta + (B_1 - B_2 D_{22}^{-1} D_{21}) u_1 + B_2 D_{22}^{-1} y_2 \\ y_1 &= (C_1 - D_{12} D_{22}^{-1} C_2)\eta + (D_{11} - D_{12} D_{22}^{-1} D_{21}) u_1 + D_{12} D_{22}^{-1} y_2 \\ u_2 &= -D_{22}^{-1} C_2 \eta - D_{22}^{-1} D_{21} u_1 + D_{22}^{-1} y_2 \end{aligned} \tag{26}$$

where η denotes the state variables of the inverted system and hence the states of the coupling numerator model.

The General Case: D_{22} Singular

The case where D_{22} is not invertible is more involved, since there exists no closed-form solution for the channel 2 inverse. Instead an algorithmic procedure can be given to compute the suitable matrices needed to invert the input-output behavior of channel 2. The outcome of this procedure depends on the input-output pairings and on their respective relative degrees. In the following, an adapted version of the infinite-zero-structure algorithm for the design of decoupling feedback controllers in time domain (Ref. 7) is proposed.

Some notation is introduced first. In the following, if applied to a vector, the index i denotes its i-th component (e.g. $y_{2,i}$ denotes the i-th component of y_2) and if applied to a matrix it denotes its i-th row (e.g. $C_{2,i}$ denotes the i-th row of C_2). In order to simplify notation in the equations that follow define

$$C_{2,i} A^{-1} B_l := D_{2l,i}, \quad l = 1,2 \tag{27}$$

This notation is unambiguous because no inverse of A occurs in this context. The relative degree of input u_l with respect to output y_2 is defined by

$$r_{l,i} = \min\{d = 0,1,2,\ldots \mid C_{2,i} A^{d-1} B_l \neq 0\}, \quad l = 1,2 \tag{28}$$

and coincides with the derivative order of $y_{2,i}$ in which the input u_l appears for the first time. It is a measure for the amount of lag between inputs and outputs due to integrators. For example, a relative degree of zero means there is a direct feedthrough from input to output, a relative degree of two means the input is integrated two times until affecting the output. The derivative of $y_{2,i}$ is denoted by $y_{2,i}^{(d)}$ where $d = 0,1,2\ldots$ is the derivative order. The vector relative degree is given by

$$r_l^{vec} := \begin{pmatrix} r_{l,1} & \cdots & r_{l,n_2} \end{pmatrix}, \quad l = 1,2 \tag{29}$$

The key idea to obtaining an expression for the channel 2 inverse is to differentiate output y_2 until input u_2 appears in the equations. Consider the i-th row of eq. (25). Its derivatives are given by

$$y_{2,i}^{(d)} = C_{2,i} A^d x + \sum_{k=r_{1,i}}^{d} C_{2,i} A^{k-1} B_1 u_1^{(d-k)} \tag{30}$$

if $d < r_{2,i}$ and

$$y_{2,i}^{(r_{2,i})} = C_{2,i} A^{r_{2,i}} x + \sum_{k=r_{1,i}}^{r_{2,i}} C_{2,i} A^{k-1} B_1 u_1^{(r_{2,i}-k)} + C_{2,i} A^{r_{2,i}-1} B_2 u_2 \tag{31}$$

if $d = r_{2,i}$. By convention, the sum in both expressions is zero if the upper index is less than the lower index. This is repeated for all outputs $i = 1,\ldots,n_2$ in channel 2, and then the matrix

$$D_{22}^* := \begin{pmatrix} C_{2,1} A^{r_{2,1}-1} B_2 u_2 \\ \vdots \\ C_{2,n_{y_2}} A^{r_{2,n_2}-1} B_2 u_2 \end{pmatrix} \tag{32}$$

is formed. If this matrix is invertible the equation

$$y_2^{(r)} = C_2^* x + D_{21}^* M(s) u_1 + D_{22}^* u_2 \tag{33}$$

can be solved for u_2 analogously to the third equation in (26). The definitions of C_2^*, D_{21}^*, and $M(s)$ are given in Appendix A. A second equation is needed to complete the inversion of channel 2 and is given by

$$\xi = S_1 x + RM(s) u_1 \tag{34}$$

whose components ξ, S_1, and R are defined in Appendix A as well. A suitable state transformation allows to reduce the order of the resulting dynamic system. To that end, choose S_2 such that the matrix $S^T := \begin{pmatrix} S_1^T & S_2^T \end{pmatrix}$ is invertible with inverse $S^{-1} =: T = \begin{pmatrix} T_1 & T_2 \end{pmatrix}$. The state transformation is defined by

$$Sx = \begin{pmatrix} S_1 x \\ S_2 x \end{pmatrix} = \begin{pmatrix} \xi - RM(s) u_1 \\ \eta \end{pmatrix} \tag{35}$$

or, equivalently,

$$x = T \begin{pmatrix} \xi - RM(s) u_1 \\ \eta \end{pmatrix} = T_1 (\xi - RM(s) u_1) + T_2 \eta \tag{36}$$

where η denotes the dynamic states of the reduced-order inverse system.

After plugging the expression for u_2 from eq. (33) into the dynamic equation for η, applying the state transformation, and

collecting terms, the reduced-order state-space equations are given as follows

$$\begin{aligned}
\dot{\eta} &= S_2(A - B_2 D_{22}^{*-} C_2^*) T_2 \eta \\
&\quad + S_2(B_1 + (B_2 D_{22}^{*-}(C_2^* T_1 R - D_{21}^*) - A T_1 R) M(s)) u_1 \\
&\quad + S_2 \left((A - B_2 D_{22}^{*-} C_2^*) T_1 \mid B_2 D_{22}^{*-} \right) L(s) y_2 \\
y_1 &= (C_1 - D_{12} D_{22}^{*-} C_2^*) T_2 \eta \\
&\quad + (D_{11} + (D_{12} D_{22}^{*-}(C_2^* T_1 R - D_{21}^*) - C_1 T_1 R) M(s)) u_1 \\
&\quad + \left((C_1 - D_{12} D_{22}^{*-} C_2^*) T_1 \mid D_{12} D_{22}^{*-} \right) L(s) y_2 \\
u_2 &= -D_{22}^{*-} C_2^* T_2 \eta + D_{22}^{*-}(C_2^* T_1 R - D_{21}^*) M(s) u_1 \\
&\quad + \left(-D_{22}^{*-} C_2^* T_1 \mid D_{22}^{*-} \right) L(s) y_2
\end{aligned} \tag{37}$$

where D_{22}^{*-} is shorthand notation for $(D_{22}^*)^{-1}$ and the y_2 derivative filter matrix $L(s)$ is defined by

$$L(s) y_2 := \begin{pmatrix} \xi \\ \hline y_2^{(r)} \end{pmatrix} \tag{38}$$

Note that if $D_{22} = 0$ one can choose S_2 such that $S_2 B_2 = 0$. If, in addition, also $D_{11} = 0$ and $D_{12} = 0$ the equations simplify to

$$\begin{aligned}
\dot{\eta} &= S_2 A T_2 \eta + S_2(B_1 - A T_1 R M(s)) u_1 + \left(S_2 A T_1 \mid 0 \right) L(s) y_2 \\
y_1 &= C_1 T_2 \eta - C_1 T_1 R M(s) u_1 + \left(C_1 T_1 \mid 0 \right) L(s) y_2 \\
u_2 &= -D_{22}^{*-} C_2^* T_2 \eta + D_{22}^{*-}(C_2^* T_1 R - D_{21}^*) M(s) u_1 \\
&\quad + \left(-D_{22}^{*-} C_2^* T_1 \mid D_{22}^{*-} \right) L(s) y_2
\end{aligned} \tag{39}$$

The following should be noted regarding the invertibility of P_{22}: If P_{22} is a transfer function, it is invertible if it has full normal rank. This means that $P_{22}(s)$ must have full rank for all but finitely many values of s (the transmission zeros of P_{22}). However, it is not easy to find suitable criteria for general invertibility in state space in the literature, because it is often assumed that the feedthrough matrix is zero or that the relative degree is well-defined. It is clear that at least $\begin{pmatrix} B_2^T & D_{22}^T \end{pmatrix}^T$ must have full column rank and $\begin{pmatrix} C_2 & D_{22} \end{pmatrix}$ full row rank, but this is not sufficient. Rank conditions such as controllability and observability may also play a role. However, it should be noted that a minimum realization of P_{22} cannot simply be enforced by canceling out uncontrollable and unobservable modes, as otherwise the state transformation in channel 1 will no longer work. For the algorithm above, this means that in an implementation it should be checked that the row rank of S_1 is full and the algorithm should be aborted as soon as the summed vector relative degree exceeds the number of system states.

With computer algebra software at hand, the components of $Q(s)$ in eq. (9) can of course also be calculated symbolically. However, the dynamic order (i.e. the number of integrators involved) for MIMO components would then be significantly higher because the individual subcomponents would have to be realized with separate system matrices. In contrast, the above algorithm produces a common system matrix that all components share. This better reflects physical reality and significantly reduces the dynamic order for MIMO models. In addition to the structural insights it offers, this is another advantage of the above procedure.

Relation to Other Approaches

For the special case of a system where the output equals the state

$$\begin{aligned}
\begin{pmatrix} \dot{x}_1 \\ \dot{x}_2 \end{pmatrix} &= \begin{pmatrix} A_{11} & A_{12} \\ A_{21} & A_{22} \end{pmatrix} \begin{pmatrix} x_1 \\ x_2 \end{pmatrix} + \begin{pmatrix} B_{11} \\ B_{21} \end{pmatrix} u_1 + \begin{pmatrix} B_{12} \\ B_{22} \end{pmatrix} u_2 \\
y_1 &= x_1 \\
y_2 &= x_2
\end{aligned} \tag{40}$$

and where B_{22} is non-singular (i.e. with well-defined vector relative degree $r_2^{vec} = \begin{pmatrix} 1 & \cdots & 1 \end{pmatrix}$) the proposed procedure yields

$$\begin{aligned}
\dot{x}_1 &= (A_{11} - B_{12} B_{22}^{-1} A_{21}) x_1 + (B_{11} - B_{12} B_{22}^{-1} B_{21}) u_1 \\
&\quad + \left(A_{12} - B_{12} B_{22}^{-1} A_{22} \mid B_{12} B_{22}^{-1} \right) \begin{pmatrix} I \\ sI \end{pmatrix} y_2 \\
y_1 &= x_1 \\
u_2 &= -B_{22}^{-1} A_{21} x_1 - B_{22}^{-1} B_{21} u_1 + \left(-B_{22}^{-1} A_{22} \mid B_{22}^{-1} \right) \begin{pmatrix} I \\ sI \end{pmatrix} y_2
\end{aligned} \tag{41}$$

The system dynamics from u_1 to y_1 are identical to the output of the algorithm given in (Ref. 3) to compute the state-space coupling numerator model if the notation introduced here is adopted.

Example

Consider a state-space realization of the system given in eq. (20)

$$\left(\begin{array}{c|c|c} A & B_1 & B_2 \\ \hline C_1 & D_{11} & D_{12} \\ \hline C_2 & D_{21} & D_{22} \end{array} \right) = \left(\begin{array}{cccccc|cc} -2 & -1 & 0 & 0 & 0 & 2 & 0 & 0 \\ 1 & 0 & 0 & 0 & 0 & 0 & 0 & 0 \\ 0 & 0 & -5 & 0 & 0 & 1 & 0 & 0 \\ 0 & 0 & 0 & -2 & 0 & 0 & 2 & 0 \\ 0 & 0 & 0 & 0 & -2 & 0 & 0 & 2 \\ \hline 0 & 1 & 0 & 0 & .5 & 0 & 0 & 0 \\ \hline 0 & 0 & 1 & 0 & 0 & 0 & 2 & 0 \\ 0 & 0 & 0 & -1 & 1 & 0 & 2 & 0 \end{array} \right) \tag{42}$$

The feedthrough matrix D_{22} has two non-zero rows, hence, $r_{2,1} = r_{2,2} = 0$ and $D_{22}^* = D_{22}$. However, D_{22}^* is singular. Thus, the procedure given in Appendix A has to be employed. An additional output $y_{2,w}$ is constructed by choosing $y_{2,w} = w^T y_2 = \begin{pmatrix} 1 & -1 \end{pmatrix} y_2$ and is then differentiated once to obtain $r_{2,w} = 1$. The index j is arbitrarily set to $j = 2$. The

new output therefore replaces or extends the expressions derived from $y_{2,2}$ yielding

$$D_{22}^* = \begin{pmatrix} 2 & 0 \\ 2 & -2 \end{pmatrix} \tag{43}$$

as well as

$$C_2^* = \begin{pmatrix} 0 & 0 & 1 & 0 & 0 \\ 0 & 0 & -5 & -2 & 2 \end{pmatrix}, \quad D_{21}^* = \begin{pmatrix} 0 \\ 1 \end{pmatrix} \tag{44}$$

in eq. (33). Note that D_{22}^* is now invertible. Also note that $R = 0$ and $M(s) = 1$ in this case, hence, eq. (34) reads

$$y_{2,w} = \begin{pmatrix} 0 & 0 & 1 & 1 & -1 \end{pmatrix} x = S_1 x = \xi \tag{45}$$

To make the state transformation work one can choose

$$S_2 = \begin{pmatrix} 1 & 0 & 0 & 0 & 0 \\ 0 & 1 & 0 & 0 & 0 \\ 0 & 0 & 1 & 0 & 0 \\ 0 & 0 & 0 & 1 & 0 \end{pmatrix} \tag{46}$$

resulting in an inverse transformation of

$$T = \begin{pmatrix} T_1 \mid T_2 \end{pmatrix} = \left(\begin{array}{c|cccc} 0 & 1 & 0 & 0 & 0 \\ 0 & 0 & 1 & 0 & 0 \\ 0 & 0 & 0 & 1 & 0 \\ 0 & 0 & 0 & 0 & 1 \\ -1 & 0 & 0 & 1 & 1 \end{array} \right) \tag{47}$$

eventually leading to a state-space representation of Q with

$$\left(\begin{array}{c|c|c} A_{cn} & B_{cn1} & B_{cn2} \\ \hline C_{cn1} & D_{cn11} & D_{cn12} \\ \hline C_{cn2} & D_{cn21} & D_{cn22} \end{array} \right) = \left(\begin{array}{cccc|c|cccc} -2 & -1 & 0 & 0 & 2 & 0 & 0 & 0 \\ 1 & 0 & 0 & 0 & 0 & 0 & 0 & 0 \\ 0 & 0 & -5 & 0 & 1 & 0 & 0 & 0 \\ 0 & 0 & -1 & -2 & 0 & 0 & 1 & 0 \\ \hline 0 & 1 & .5 & .5 & 0 & -.5 & 0 & 0 \\ \hline 0 & 0 & -.5 & 0 & 0 & 0 & .5 & 0 \\ 0 & 0 & -2 & 0 & .5 & -1 & .5 & -.5 \end{array} \right) \tag{48}$$

where the second input is given by

$$L(s) y_2 = \begin{pmatrix} 1 & -1 \\ 1 & 0 \\ s & -s \end{pmatrix} \begin{pmatrix} y_{2,1} \\ y_{2,2} \end{pmatrix} = \begin{pmatrix} y_{2,w} \\ y_{2,1} \\ y_{2,w}^{(1)} \end{pmatrix} \tag{49}$$

Note that Q has only four states compared to the five states in eq. (42).

DYNAMIC PROPERTIES

It is clear that $Q_{22} = P_{22}^{-1}$ is realizable only if there is a non-singular direct feedthrough from u_2 to y_2, hence the introduction of the $L(s)$ filter in eq. (38) in the procedure above. The off-diagonal elements of Q are realizable only if the plant off-diagonal elements P_{12} and P_{21} have a higher relative degree than channel 2 meaning that for Q_{12} being realizable, u_2 must not act faster on y_1 than on y_2 and for Q_{21}, u_1 must not act faster on y_2 than on y_1. Since P_{11} is realizable by assumption the question whether Q_{11} is realizable or not depends on whether the lead provided by P_{22}^{-1} can be compensated by P_{12} and P_{21} or not. Non-realizable Q elements might indicate a poor choice of input-output pairs (u_1, y_1), (u_2, y_2), but can also be consequence of combining slow outputs (e.g. attitude angles or translational velocities) in y_2 with fast outputs (e.g. angular rates or accelerations) in y_1.

Remember that the determinant of a square transfer function matrix is a scalar transfer function consisting of plant zeros divided by plant poles. From eq. (16) one can hence infer that

$$\text{poles of } Q_{11} \subseteq \text{ zeros of } P_{22} \tag{50}$$

and

$$\text{zeros of } Q_{11} \subseteq \text{ zeros of } P \tag{51}$$

when P and P_{22} stem from the same realization and hence share the same poles. These subsets are usually strict due to pole-zero cancellations, but there are examples in which equality holds. These relationships remain valid if Q_{11} is non-square. Poles and zeros of the off-diagonal blocks Q_{12} and Q_{21} directly result from zeros of P_{12}, P_{21}, and P_{22}^{-1}. In a crude oversimplification one might therefore write

$$\begin{pmatrix} Q_{11} & Q_{12} \\ Q_{21} & Q_{22} \end{pmatrix} \text{“} = \text{“} \begin{pmatrix} \frac{\text{“zeros of } P\text{”}}{\text{“zeros of } P_{22}\text{”}} & \frac{\text{“zeros of } P_{12}\text{”}}{\text{“zeros of } P_{22}\text{”}} \\ \frac{\text{“zeros of } P_{21}\text{”}}{\text{“zeros of } P_{22}\text{”}} & \frac{\text{“poles of } P\text{”}}{\text{“zeros of } P_{22}\text{”}} \end{pmatrix} \tag{52}$$

Example

Note that P_{22} in eq. (20) has one pole at $s = -2$ and no transmission zeros. If, however, it is realized by $P_{22} = C_2(sI - A)^{-1}B_2 + D_{22}$ with the matrices given in eq. (42) it has poles at $s = \{-1, -1, -2, -2, -5\}$ and zeros at $s = \{-1, -1, -2, -5\}$. The whole plant P has poles at the same location but its zeros amount to $s = \{-1.934, -2.533 \pm 3.845i\}$. Hence, Q_{11} has zeros at the same location but poles only at $s = \{-1, -1, -2, -5\}$ which coincides with the expression for Q_{11} in eq. (22) since no pole-zero cancellation occurs.

APPLICATION TO CONTROLLER DESIGN

Coupling numerator models provide insight into the dynamics of a controlled MIMO system and can assist in deriving an initial, feasible controller design. In this section, it is assumed that P_{11} is also square and invertible. Applying the previously presented method now with reversed roles for both channels leads to

$$\begin{aligned} \begin{pmatrix} u_1 \\ y_2 \end{pmatrix} &= \begin{pmatrix} P_{11}^{-1} & -P_{11}^{-1}P_{12} \\ P_{21}P_{11}^{-1} & P_{22} - P_{21}P_{11}^{-1}P_{12} \end{pmatrix} \begin{pmatrix} r_1 \\ u_2 \end{pmatrix} \\ &=: \begin{pmatrix} R_{11} & R_{12} \\ R_{21} & R_{22} \end{pmatrix} \begin{pmatrix} r_1 \\ u_2 \end{pmatrix} \end{aligned} \tag{53}$$

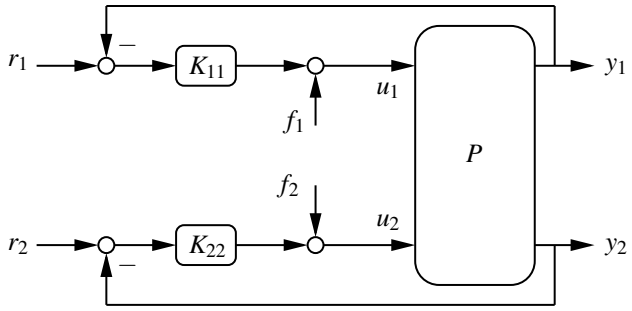

Figure 2: Two-degrees-of-freedom controller structure without decoupling

No Decoupling Crossfeeds

Consider the controlled plant in Fig. 2 with reference signals r_1 and r_2, feedback controllers K_{11} and K_{22}, and feedforward signals f_1 and f_2. To obtain an initial, feasible controller for the plant P, the controllers K_{11} and K_{22} are designed to stabilize the following idealized dynamics

$$\begin{pmatrix} y_1 \\ y_2 \end{pmatrix} = \begin{pmatrix} Q_{11}K_{11} & 0 \\ 0 & R_{22}K_{22} \end{pmatrix} \begin{pmatrix} r_1 - y_1 \\ r_2 - y_2 \end{pmatrix} + \begin{pmatrix} 0 & Q_{12} \\ R_{21} & 0 \end{pmatrix} \begin{pmatrix} r_1 \\ r_2 \end{pmatrix} + \begin{pmatrix} Q_{11} & 0 \\ 0 & R_{22} \end{pmatrix} \begin{pmatrix} f_1 \\ f_2 \end{pmatrix} \tag{54}$$

Since both channels are decoupled, the controllers K_{11} and K_{22} can be designed independently of each other. The feedback controller K_{11} is designed to achieve stabilization and good performance for Q_{11}. The reference crossfeed of channel 2 $Q_{12}r_2$ can be considered as a disturbance acting on y_1. This "disturbance" will be rejected and hence decoupling of channel 2 will be achieved if the closed-loop transfer function

$$(I + Q_{11}K_{11})^{-1}Q_{12} \tag{55}$$

is small. This is usually the case for frequencies up to the controller bandwidth where the closed-loop sensitivity $(I + Q_{11}K_{11})^{-1}$ is small.

The tracking performance can be further improved by employing a feedforward controller such as, for example, $f_1 = Q_{11}^{-1}r_1$. Suppressing the channel 2 cross-coupling in addition to providing good tracking performance can be achieved by choosing $f_1 = Q_{11}^{-1}(r_1 - Q_{12}r_2)$. The feedback controller K_{22} and the feedforward controller f_2 are designed analogously.

In order to establish a connection between the actual controlled plant and the coupling numerator models, the closed-loop dynamics are rearranged appropriately. According to Fig. 2 one has

$$\begin{pmatrix} y_1 \\ y_2 \end{pmatrix} = \begin{pmatrix} P_{11} & P_{12} \\ P_{21} & P_{22} \end{pmatrix} \left(\begin{pmatrix} K_{11} & 0 \\ 0 & K_{22} \end{pmatrix} \begin{pmatrix} r_1 - y_1 \\ r_2 - y_2 \end{pmatrix} + \begin{pmatrix} f_1 \\ f_2 \end{pmatrix} \right)$$
$$\begin{pmatrix} u_1 \\ u_2 \end{pmatrix} = \begin{pmatrix} K_{11} & 0 \\ 0 & K_{22} \end{pmatrix} \left(\begin{pmatrix} r_1 \\ r_2 \end{pmatrix} - \begin{pmatrix} P_{11} & P_{12} \\ P_{21} & P_{22} \end{pmatrix} \begin{pmatrix} u_1 \\ u_2 \end{pmatrix} \right) + \begin{pmatrix} f_1 \\ f_2 \end{pmatrix} \tag{56}$$

The equation for y_1 can be solved for y_1 and the result is inserted into the equation for y_2. The equation for u_1 is solved for u_1, but the dependency on u_2 is retained. The same is done vice versa for y_2 and u_2. Then, the resulting closed-loop dynamics can be expressed as follows

$$\begin{pmatrix} y_1 \\ y_2 \end{pmatrix} = \begin{pmatrix} \tilde{Q}_{11}K_{11} & 0 \\ 0 & \tilde{R}_{22}K_{22} \end{pmatrix} \begin{pmatrix} r_1 - y_1 \\ r_2 - y_2 \end{pmatrix} + \begin{pmatrix} 0 & \tilde{Q}_{12} \\ \tilde{R}_{21} & 0 \end{pmatrix} \begin{pmatrix} r_1 \\ r_2 \end{pmatrix} + \begin{pmatrix} \tilde{Q}_{11} & P_{12}(I + K_{22}P_{22})^{-1} \\ P_{12}(I + K_{11}P_{11})^{-1} & \tilde{R}_{22} \end{pmatrix} \begin{pmatrix} f_1 \\ f_2 \end{pmatrix}$$
$$\begin{pmatrix} u_1 \\ u_2 \end{pmatrix} = \begin{pmatrix} 0 & \tilde{R}_{12} \\ \tilde{Q}_{21} & 0 \end{pmatrix} \begin{pmatrix} u_1 \\ u_2 \end{pmatrix} + \begin{pmatrix} \tilde{R}_{11} & 0 \\ 0 & \tilde{Q}_{22} \end{pmatrix} \begin{pmatrix} r_1 \\ r_2 \end{pmatrix} + \begin{pmatrix} (I + K_{11}P_{11})^{-1} & 0 \\ 0 & (I + K_{22}P_{22})^{-1} \end{pmatrix} \begin{pmatrix} f_1 \\ f_2 \end{pmatrix} \tag{57}$$

where

$$\begin{aligned} \tilde{Q}_{11} &= P_{11} - P_{12}K_{22}(I + P_{22}K_{22})^{-1}P_{21} \\ \tilde{R}_{22} &= P_{22} - P_{21}K_{11}(I + P_{11}K_{11})^{-1}P_{12} \\ \tilde{Q}_{12} &= P_{12}(I + K_{22}P_{22})^{-1}K_{22} \\ \tilde{R}_{21} &= P_{21}(I + K_{11}P_{11})^{-1}K_{11} \\ \tilde{Q}_{21} &= -(I + K_{22}P_{22})^{-1}K_{22}P_{21} \\ \tilde{R}_{12} &= -(I + K_{11}P_{11})^{-1}K_{11}P_{12} \\ \tilde{Q}_{22} &= (I + K_{22}P_{22})^{-1}K_{22} \\ \tilde{R}_{11} &= (I + K_{11}P_{11})^{-1}K_{11} \end{aligned} \tag{58}$$

are (usually low- to mid-frequency) approximations of the coupling numerator models in eqs. (9) and (53). The idea of the coupling numerator design method is based on the observation that if the designed controllers K_{11} and K_{22} are robust enough in the first place, they will also stabilize the actual plant P since $\tilde{Q}_{11} \approx Q_{11}$ and $\tilde{R}_{22} \approx R_{22}$.

Note that if feedforward controllers are used for both channels they introduce additional crossfeeds which depend on the other channel's controller. In this case, one might have to iterate the design to mitigate the coupling effect introduced by the feedforward controllers. If only one feedforward controller is employed, a sequential design is still feasible.

One strategy for improving closed-loop decoupling is to increase the bandwidth of the controllers K_{11} and K_{22} in accordance with expression (55). However, this means that measurement noise suppression gets worse and actuator activity increases – effects that are rather undesirable in practice. A better strategy would be to improve the decoupling by introducing controller crossfeeds. This is discussed in more detail in the next two subsections.

Partial Decoupling With One Crossfeed

To improve the decoupling in the closed loop, a crossfeed K_{21} from u_1 to u_2 can be added to the controller output, see Fig. 3.

By selecting $K_{21} = Q_{21} = -P_{22}^{-1}P_{21}$, perfect decoupling of channel 2 from channel 1 is achieved. An analogous procedure as explained above then shows that the closed-loop dy-

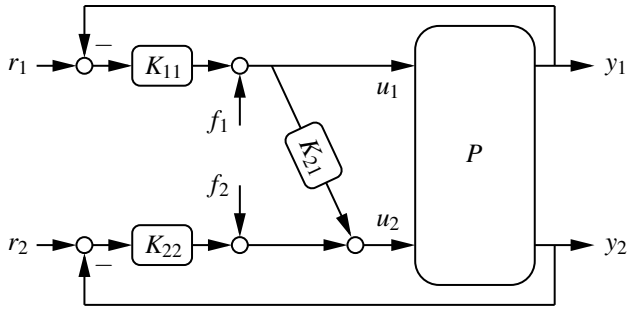

Figure 3: Two-degrees-of-freedom controller structure with partial decoupling

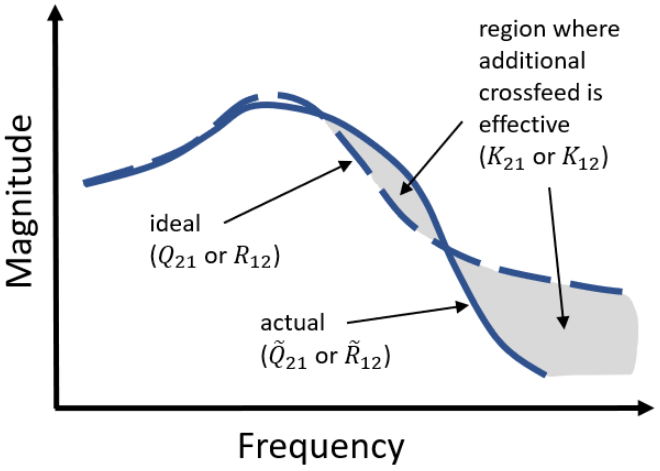

Figure 4: Effective region of an additional controller crossfeed

namics are equivalent to

$$\begin{aligned}\begin{pmatrix}y_1\\y_2\end{pmatrix} &= \begin{pmatrix}Q_{11}K_{11} & 0\\0 & P_{22}K_{22}\end{pmatrix}\begin{pmatrix}r_1-y_1\\r_2-y_2\end{pmatrix}+\begin{pmatrix}0 & \tilde{Q}_{12}\\0 & 0\end{pmatrix}\begin{pmatrix}r_1\\r_2\end{pmatrix}\\ &\quad+\begin{pmatrix}Q_{11} & P_{12}(I+K_{22}P_{22})^{-1}\\0 & P_{22}\end{pmatrix}\begin{pmatrix}f_1\\f_2\end{pmatrix}\\ \begin{pmatrix}u_1\\u_2\end{pmatrix} &= \begin{pmatrix}0 & \tilde{R}_{12}\\Q_{21} & 0\end{pmatrix}\begin{pmatrix}u_1\\u_2\end{pmatrix}+\begin{pmatrix}\tilde{R}_{11} & 0\\0 & \tilde{Q}_{22}\end{pmatrix}\begin{pmatrix}r_1\\r_2\end{pmatrix}\\ &\quad+\begin{pmatrix}(I+K_{11}P_{11})^{-1} & 0\\0 & (I+K_{22}P_{22})^{-1}\end{pmatrix}\begin{pmatrix}f_1\\f_2\end{pmatrix}\end{aligned} \tag{59}$$

As one can see, there is no longer any influence of r_1 on y_2. The coupling term $\tilde{R}_{21}$ has completely disappeared from the equation for y_2 in (59). At the same time, the dynamics in channel 2 are no longer determined by $\tilde{R}_{22}$ but by P_{22}. This also means that a preliminary design of K_{22} based on R_{22} may no longer be suitable for controlling the decoupled plant (i.e. P_{22}). Furthermore, it can be observed that the crossfeed from u_1 to u_2 is now exactly Q_{21}. The equations for channel 1 now contain Q_{11} instead of $\tilde{Q}_{11}$, but apart from that remain unchanged.

Perfect decoupling is rather unsuitable for practical implementation because it is susceptible to model errors and uncertainties. In practice, K_{21} is chosen such that it only matches Q_{21} locally in a selected frequency range. One can make use

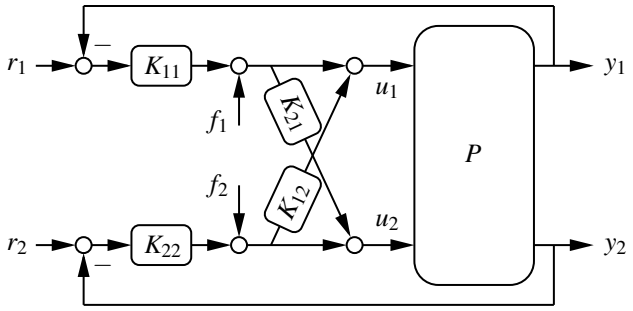

Figure 5: Two-degrees-of-freedom controller structure with full decoupling in forward configuration

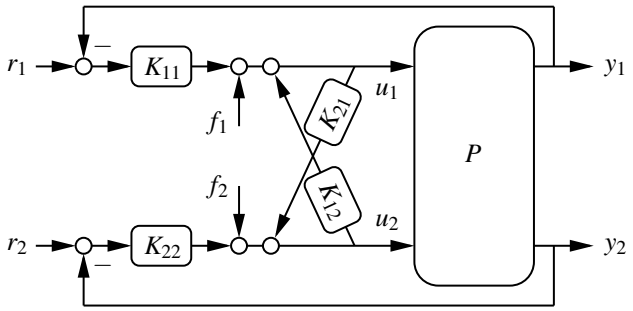

Figure 6: Two-degrees-of-freedom controller structure with full decoupling in reverse configuration

of the fact that the controller already automatically decouples the low-frequency plant dynamics, see Fig. 4. A K_{21} selected in this way can be viewed as an interpolation between the case with no decoupling in eq. (57) and the case with perfect decoupling in eq. (59). The equations in Appendix B make this interpolation property explicit.

Full Decoupling With Two Crossfeeds

When using two crossfeeds K_{12} and K_{21}, there are two ways to implement them symmetrically: in forward configuration, see Fig. 5, and in reverse configuration, see Fig. 6. It should be mentioned that the feedforward signals could also be added after the decoupling elements. However, they would then no longer benefit from the decoupling structure and would in turn cause crossfeeds again. This option is therefore not discussed further here. For perfect decoupling, the crossfeeds must satisfy $K_{12} = R_{12} = -P_{11}^{-1}P_{12}$ and $K_{21} = Q_{21} = -P_{22}^{-1}P_{21}$. In the forward configuration this leads to

$$\begin{aligned}\begin{pmatrix}y_1\\y_2\end{pmatrix} &= \begin{pmatrix}Q_{11}K_{11} & 0\\0 & R_{22}K_{22}\end{pmatrix}\begin{pmatrix}r_1-y_1\\r_2-y_2\end{pmatrix}+\begin{pmatrix}Q_{11} & 0\\0 & R_{22}\end{pmatrix}\begin{pmatrix}f_1\\f_2\end{pmatrix}\\ \begin{pmatrix}u_1\\u_2\end{pmatrix} &= \begin{pmatrix}0 & R_{12}\\Q_{21} & 0\end{pmatrix}\begin{pmatrix}u_1\\u_2\end{pmatrix}\\ &\quad+\begin{pmatrix}XK_{11} & 0\\0 & P_{22}^{-1}R_{22}(I+K_{22}R_{22})^{-1}K_{22}\end{pmatrix}\begin{pmatrix}r_1\\r_2\end{pmatrix}\\ &\quad+\begin{pmatrix}X & 0\\0 & P_{22}^{-1}R_{22}(I+K_{22}R_{22})^{-1}\end{pmatrix}\begin{pmatrix}f_1\\f_2\end{pmatrix}\end{aligned} \tag{60}$$

where

$$X := P_{11}^{-1}Q_{11}(I+K_{11}Q_{11})^{-1} \tag{61}$$

Note that the reference crossfeeds on y_1 and y_2 are eliminated and that the dynamics seen by the controllers are exactly Q_{11} and R_{22}. Further, note that the transfer functions from r_1 to u_1 and r_2 to u_2 are still approximately P_{11}^{-1} and P_{22}^{-1}.
Employing the reverse configuration for decoupling according to Fig. 6 with the same crossfeeds as above leads to

$$\begin{pmatrix} y_1 \\ y_2 \end{pmatrix} = \begin{pmatrix} P_{11}K_{11} & 0 \\ 0 & P_{22}K_{22} \end{pmatrix} \begin{pmatrix} r_1 - y_1 \\ r_2 - y_2 \end{pmatrix} + \begin{pmatrix} P_{11} & 0 \\ 0 & P_{22} \end{pmatrix} \begin{pmatrix} f_1 \\ f_2 \end{pmatrix}$$
$$\begin{pmatrix} u_1 \\ u_2 \end{pmatrix} = \begin{pmatrix} 0 & R_{12} \\ Q_{21} & 0 \end{pmatrix} \begin{pmatrix} u_1 \\ u_2 \end{pmatrix} + \begin{pmatrix} \tilde{R}_{11} & 0 \\ 0 & \tilde{Q}_{22} \end{pmatrix} \begin{pmatrix} r_1 \\ r_2 \end{pmatrix} + \begin{pmatrix} (I + K_{11}P_{11})^{-1} & 0 \\ 0 & (I + K_{22}P_{22})^{-1} \end{pmatrix} \begin{pmatrix} f_1 \\ f_2 \end{pmatrix} \tag{62}$$

Here it can be seen that the reference crossfeeds are also eliminated, but this time the dynamics of the decoupled system correspond to the diagonal elements of the actual plant P_{11} and P_{22}.
The forward configuration is the structure used more frequently in practice and it fits in with the idea of using Q_{11} and R_{22} as the basis for the design of K_{11} and K_{22}. The reverse configuration seems to have been used mainly in the control of industrial processes, see (Ref. 8) and the references therein. According to (Ref. 8), the advantages of the reverse configuration are the consideration of actuator limitation in the decoupling and a simplified switching between controlled and uncontrolled processes. However, possible stability problems when using this configuration are also pointed out, which is why a partial decoupling structure is recommended whenever possible.

A Heuristic Procedure for Initial MIMO Controller Design

The choice of the decoupling structure has an impact on which dynamics the controllers see and consequently on how they must be designed. This also applies to the design of the feedforward controllers and can be handled in two ways: Either the crossfeeds are absorbed into the plant dynamics leading to new coupling numerator models for a new controller design. Or the already designed controller is iterated directly on the basis of the actual, decoupled dynamics. Thus, the following procedure for deriving an initial, feasible controller design is suggested

1. Design K_{11} such that it stabilizes Q_{11} and the closed-loop exhibits good performance. Repeat with K_{22} for channel 2. Plug K_{11} and K_{22} into the plant P and verify that they also stabilize $\tilde{Q}_{11}$ and $\tilde{R}_{22}$.

2. Examine whether the desired level of decoupling is achieved by looking at $(I + \tilde{Q}_{11}K_{11})^{-1}\tilde{Q}_{12}$ and other performance metrics, for example, responses to step or doublet inputs. If decoupling is not satisfactory pick an appropriate decoupling structure and choose the decoupling crossfeed K_{21} to be close to Q_{21} at frequencies where improved decoupling is desired. Repeat for channel 2. Consider retuning K_{11} and K_{22} based on the resulting decoupled dynamics since they might have changed significantly compared to Q_{11} and R_{22}. Plug K_{11} and K_{22} into the plant P and verify that they also stabilize $\tilde{Q}_{11}$ and $\tilde{R}_{22}$. Repeat step 2 if necessary.

3. To further improve the performance, choose a feedforward controller depending on decoupling structure and frequency range where additional lead is desired. Plug the feedforward controller into the plant P and retune K_{11} and K_{22} based on $\tilde{Q}_{11}$ and $\tilde{R}_{22}$ if necessary.

However, it must be noted that MIMO design criteria are not taken into account with this approach. For example, the simultaneous occurrence of uncertainties in several axes must be checked in further validation and design steps and the robustness of the controller must be improved if necessary.

EXAMPLE APPLICATION: CONTROLLER DESIGN FOR A HELICOPTER IN HOVER

The general approach to controller design using constrained input/output dynamics will be briefly illustrated with the design of an Attitude-Command/Attitude-Hold controller for a helicopter in hover. It is well-known that the pitch-due-to-roll and roll-due-to-pitch couplings of helicopters are usually not negligible. A good decoupling of the pitch and roll response in hover is of particular interest. The hover model employed in this example was obtained by system identification of DLR's research helicopter ACT/FHS (Active Control Technology/Flying Helicopter Simulator) and is described and derived in detail in (Ref. 9). The model used for controller design

$$\begin{aligned} \dot{x} &= Ax + Bu \\ y &= Cx + Du \end{aligned} \tag{63}$$

has the four inputs δ_x (longitudinal cyclic), δ_y (lateral cyclic), δ_p (pedal) and δ_0 (collective), a total of 17 states (including inflow/coning, flapping and engine dynamics), and its output vector used in this example contains pitch, roll and yaw rate (q, p, r) as well the attitude angles ϕ and θ.
The controller structure used for this example is deliberately kept simple. Thus, the control of the vertical axis is neglected. The controllers for the other three axes have an identical structure: All three have a first-order prefilter that generates the reference signal for error feedback. A proportional–integral–derivative (PID) controller is used to control the pitch and roll axes, and a PI controller is used to control the yaw axis. The roll axis also contains a notch filter to suppress the lead-lag frequency. All three controllers were designed using coupling numerator models.

Figs. 7 and 8 show the respective axis dynamics for the pitch and roll axis. As can be seen, the prediction of the coupling numerator models is quite accurate. The coupling numerator models and the dynamics in the partially closed loop almost

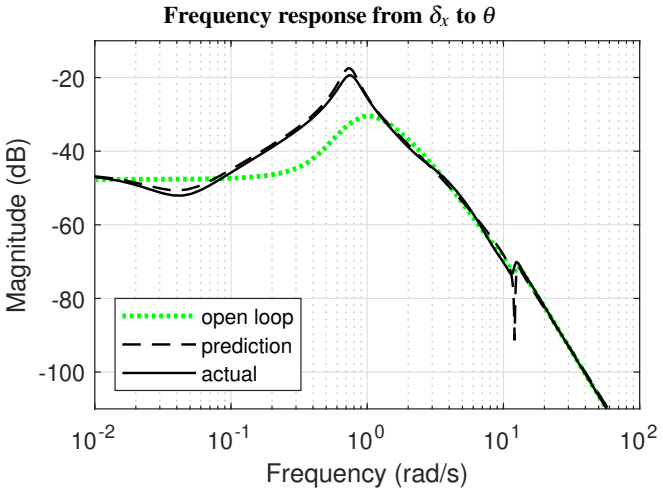

Figure 7: Pitch axis dynamics in open and partially closed loop ($\delta_y \to \phi$, $\delta_p \to r$)

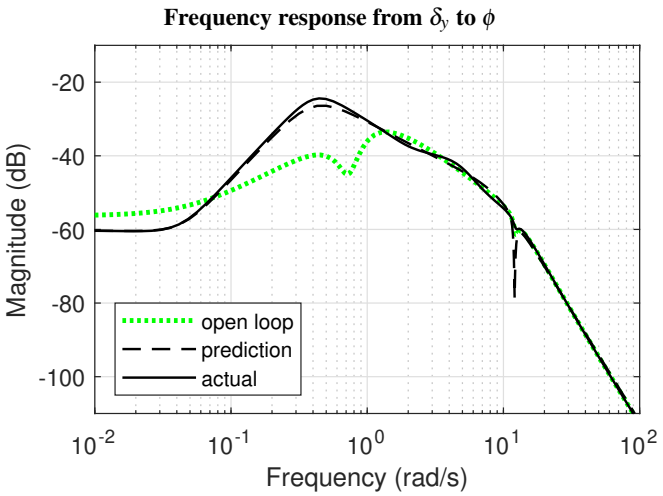

Figure 8: Roll axis dynamics in open and partially closed loop ($\delta_x \to \theta$, $\delta_p \to r$)

coincide. Furthermore, it can be seen that these dynamics deviate significantly from those of the open loop in the low to medium frequency range. The unconstrained on-axis plant dynamics would therefore be unsuitable for controller design.

Figs. 9 and 10 show the reference cross-couplings for both axes. The predicted cross-couplings agree well with the actual ones up to the controller bandwidth of approximately 1 rad/s, after which they diverge. The blue line shows the frequency response in the closed loop. As can be seen here, the coupling effects are more pronounced in the roll axis and are not suppressed in the $3-8$ rad/s range.

Figs. 11 and 12 show the control crossfeeds. The dashed lines depict the ideal controller crossfeeds needed to perfectly decouple the plant. The solid lines depict the effective actual crossfeeds established by the feedback controllers. Ideal and actual crossfeeds are identical up to around 1 rad/s. Beyond this frequency, they diverge, which results in poorer decoupling performance.

Finally, Figs. 13 and 14 show the system responses to a doublet signal with a period of 2 s and a control amplitude of 20 %.

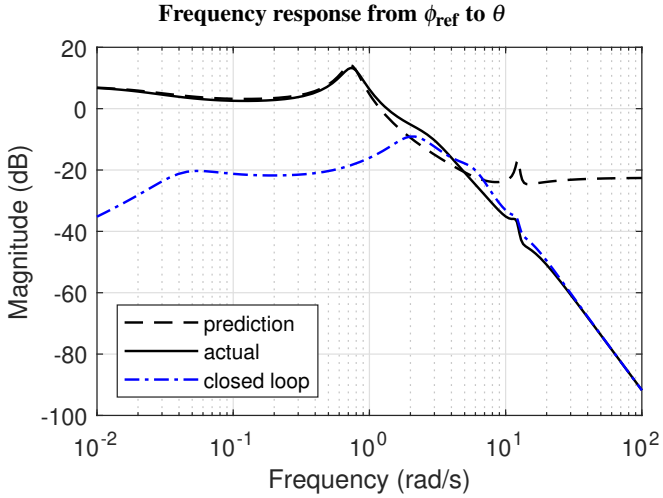

Figure 9: Reference cross-couplings for pitch axis in closed and partially closed loop ($\delta_y \to \phi$, $\delta_p \to r$)

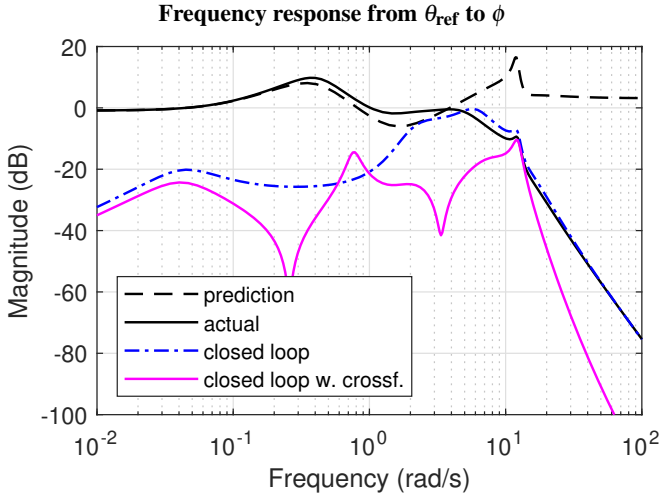

Figure 10: Reference cross-couplings for roll axis in closed and partially closed loop ($\delta_x \to \theta$, $\delta_p \to r$)

Again, it can be observed that the cross-couplings in the roll axis are much more pronounced.

To mitigate the cross-couplings in the roll axis, an additional crossfeed from δ_x to δ_y was applied. This crossfeed is designed in such a way that it corresponds approximately to the ideal crossfeed in Fig. 12 around the range of 1 rad/s. The effectiveness of the crossfeed can be checked by looking at the magenta lines in Figs. 10 and 14. They show that the crossfeed does indeed effectively suppress the cross-couplings.

CONCLUSIONS

Coupling numerator models and their extension presented herein are a versatile tool for analyzing and controlling MIMO systems. They enable a better understanding of the complex internal relationships and effects in a MIMO system and they allow to derive preliminary controller structures for the control of MIMO systems based one a decentralized one-loop-at-a-time approach. The most important results of this work can be summarized as follows

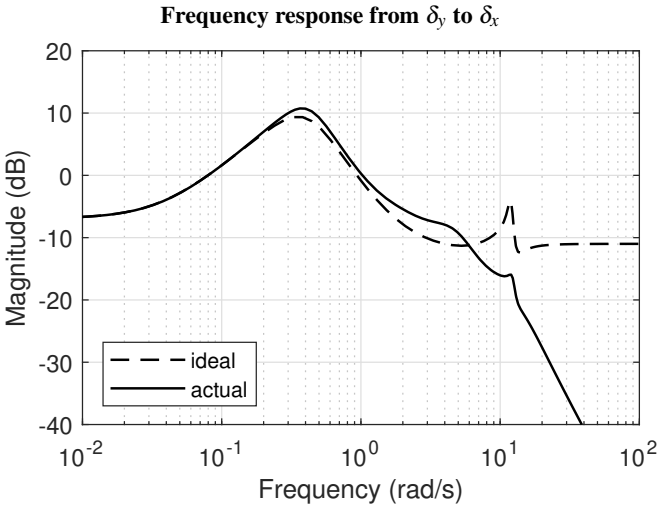

Figure 11: Crossfeed from lateral to logitudinal cyclic controls in partially closed loop ($\delta_x \to \theta$, $\delta_p \to r$)

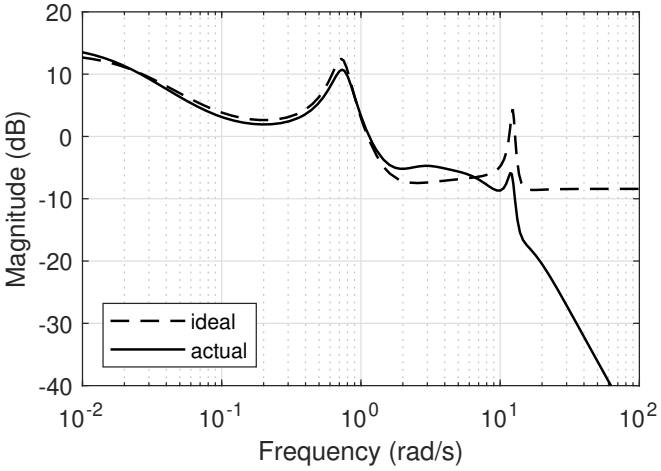

Figure 12: Crossfeed from longitudinal to lateral cyclic controls in partially closed loop ($\delta_y \to \phi$, $\delta_p \to r$)

1. The presented approach to computing coupling numerator models unifies and extends existing approaches from literature. It directly applies to the computation of constrained MIMO dynamics. Decoupling crossfeeds follow naturally from this approach.

2. Furthermore, the approach adds output references to the calculation which proves to be helpful in system analysis of the controlled system and validation of the decoupling design.

3. A general procedure is presented to derive the coupling numerator models, related crossfeed models, and the inverse of the constrained subsystem in a common state-space description.

4. The proposed coupling numerator model structure fits well into the analysis of closed-loop system dynamics. A discussion of different decoupling architectures is provided together with an interpretation of the effects of decoupling as well as a controller design guideline.

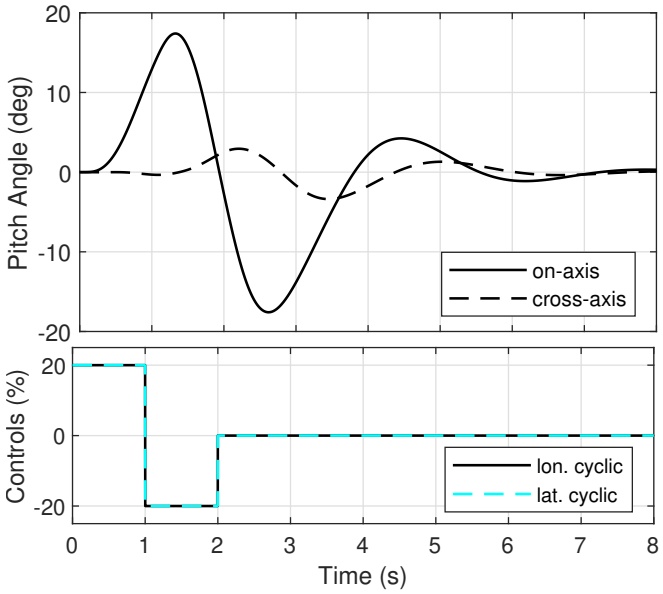

Figure 13: Pitch response to doublet input in closed loop

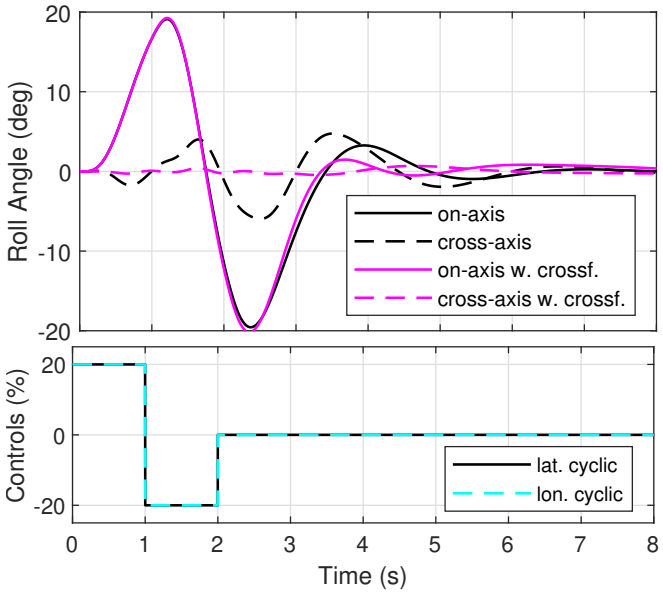

Figure 14: Roll response to doublet input in closed loop

Author contact: Frederik A. Döring, frederik.doering@dlr.de

APPENDIX A

Matrix and Vector Definitions

Two types of matrices are compiled in order to be able to conveniently write down all the equations required to calculate the coupling numerator state-space model: matrices resulting from eq. (31) to perform the actual channel 2 inversion and matrices resulting from eq. (30) to perform a state transformation that eliminates unnecessary internal states in the inverse system. Define

$$C_2^* := \begin{pmatrix} C_{2,1}A^{r_{2,1}} \\ \vdots \\ C_{2,n_2}A^{r_{2,n_2}} \end{pmatrix} \tag{64}$$

$$D_{21}^* := \begin{pmatrix} C_{2,1}A^{r_{1,1}-1}B_1 & \cdots & C_{2,1}A^{r_{2,1}-1}B_1 & N_1^1 \\ \vdots & & \vdots & \vdots \\ C_{2,n_2}A^{r_{1,n_2}-1}B_1 & \cdots & C_{2,n_2}A^{r_{2,n_2}-1}B_1 & N_{n_2}^1 \end{pmatrix} \tag{65}$$

where

$$N_i^1 := 0_{1\times(r_{max}-(r_{2,i}-r_{1,i}))}, \quad i = 1,\ldots,n_2 \tag{66}$$

and let the order of the highest u_1 derivative appearing in the equations be denoted by

$$r_{max} = \max\left(\{r_{2,i}-r_{1,i} | i = 1,\ldots,n_2\}\cup\{0\}\right) \tag{67}$$

The u_1 derivatives are accounted for by employing a derivative filter

$$M(s)^T := \begin{pmatrix} I & sI & \cdots & s^{r_{max}}I \end{pmatrix} \tag{68}$$

Note that if $r_{2,i} < r_{1,i}$ the i-th row in D_{21}^* is zero. If this is true for all $i = 1,\ldots,n_2$ then $D_{21}^* = 0_{n_2\times n_1}$. Defining

$$y_2^{(r)} := \begin{pmatrix} y_{2,1}^{(r_{2,1})} & \cdots & y_{2,n_2}^{(r_{2,n_2})} \end{pmatrix}^T \tag{69}$$

one obtains the output equation

$$y_2^{(r)} = C_2^* x + D_{21}^* M(s) u_1 + D_{22}^* u_2 \tag{70}$$

which can be solved for u_2 analogously to the third equation in (26). Using the following definitions,

$$\begin{aligned} \xi^T &:= \begin{pmatrix} y_{2,1} & \cdots & y_{2,1}^{(r_{2,1}-1)} & \cdots & y_{2,n_2} & \cdots & y_{2,n_2}^{(r_{2,n_2}-1)} \end{pmatrix} \\ S_1^T &:= \begin{pmatrix} C_{2,1}^T & \cdots & (C_{2,1}A^{r_{2,1}-1})^T & \cdots & C_{2,n_2}^T & \cdots & (C_{2,n_2}A^{r_{2,n_2}-1})^T \end{pmatrix} \\ R_i &:= \left(\begin{array}{ccc|c} & N_i^2 & & N_i^3 \\ \hline C_{2,i}A^{r_{1,i}-1}B_1 & & 0 & \\ \vdots & \ddots & & N_i^4 \\ C_{2,i}A^{r_{2,i}-2}B_1 & \cdots & C_{2,i}A^{r_{1,i}-1}B_1 & \end{array}\right) \end{aligned} \tag{71}$$

where

$$\begin{aligned} N_i^2 &:= 0_{r_{1,i}\times(r_{2,i}-r_{1,i})}, \\ N_i^3 &:= 0_{r_{1,i}\times(r_{max}-(r_{2,i}-r_{1,i}))}, \\ N_i^4 &:= 0_{(r_{2,i}-r_{1,i})\times(r_{max}-(r_{2,i}-r_{1,i}))}, \quad i = 1,\ldots,n_2 \end{aligned} \tag{72}$$

and

$$R^T := \begin{pmatrix} R_1^T & \cdots & R_{n_2}^T \end{pmatrix} \tag{73}$$

eq. (30) can be rewritten as

$$\xi = S_1 x + RM(s)u_1 \tag{74}$$

Note that outputs $y_{2,i}$ with $r_{2,i} = 0$ appear only in eq. (70) but not in eq. (74).

The Case Where D_{22}^* Is Singular

In the case where D_{22}^* is not invertible (referred to in the literature as the system having a degenerate or not well-defined relative degree), an additional output variable needs to be constructed in order to continue. In that case, there exists a non-zero vector w such that $w^T D_{22}^* = 0$. As a result, the new output variable $y_{2,w} := w^T y_2^{(r)}$ no longer depends on u_2 and can be further differentiated until u_2 appears in the derivative expressions again. According to (Ref. 7) this output derivative $y_{2,w}^{(r_{2,w})}$ then replaces $y_{2,j}^{(r_{2,j})}$ in eq. (70) where $j = \text{argmax}_{i=1\ldots n_2}\{r_i \,|\, w_i \neq 0\}$. The derivatives $y_{2,w}^{(d)}$ with $d = 0,\ldots,r_{2,w}-1$ are appended to the set of equations in (74) where the matrices therein are updated with new rows accordingly. The resulting relative degrees $r_{2,w}$ and $r_{1,w}$ are added to the respective vector relative degrees at the index j. This process is repeated until the resulting D_{22}^* is non-singular.

APPENDIX B

The general case of partial decoupling according to Fig. 3 for an unspecified, variable crossfeed K_{21} is given by

$$\begin{aligned} \begin{pmatrix} y_1 \\ y_2 \end{pmatrix} &= \begin{pmatrix} \bar{Q}_{11}K_{11} & 0 \\ 0 & \bar{R}_{22}K_{22} \end{pmatrix}\begin{pmatrix} r_1 - y_1 \\ r_2 - y_2 \end{pmatrix} + \begin{pmatrix} 0 & \tilde{Q}_{12} \\ \bar{R}_{21} & 0 \end{pmatrix}\begin{pmatrix} r_1 \\ r_2 \end{pmatrix} \\ &\quad + \begin{pmatrix} \bar{Q}_{11} & P_{12}(I+K_{22}P_{22})^{-1} \\ (P_{12}+P_{22}K_{21})Y & \bar{R}_{22} \end{pmatrix}\begin{pmatrix} f_1 \\ f_2 \end{pmatrix} \\ \begin{pmatrix} u_1 \\ u_2 \end{pmatrix} &= \begin{pmatrix} 0 & \tilde{R}_{12} \\ \bar{Q}_{21} & 0 \end{pmatrix}\begin{pmatrix} u_1 \\ u_2 \end{pmatrix} + \begin{pmatrix} \tilde{R}_{11} & 0 \\ 0 & \tilde{Q}_{22} \end{pmatrix}\begin{pmatrix} r_1 \\ r_2 \end{pmatrix} \\ &\quad + \begin{pmatrix} (I+K_{11}P_{11})^{-1} & 0 \\ 0 & (I+K_{22}P_{22})^{-1} \end{pmatrix}\begin{pmatrix} f_1 \\ f_2 \end{pmatrix} \end{aligned} \tag{75}$$

where

$$\begin{aligned} Y &= (I+K_{11}(P_{11}+P_{12}K_{21}))^{-1} \\ \bar{Q}_{11} &= P_{11} - P_{12}(I+K_{22}P_{22})^{-1}(K_{22}P_{21}-K_{21}) \\ \bar{R}_{22} &= P_{22} - (P_{21}+P_{22}K_{21})YK_{11}P_{12} \\ \bar{R}_{21} &= (P_{21}+P_{22}K_{21})YK_{11} \\ \bar{Q}_{21} &= -(I+K_{22}P_{22})^{-1}(K_{22}P_{21}-K_{21}) \end{aligned} \tag{76}$$

Note that the following interpolation properties hold: For $K_{21} = 0$ one has $\bar{Q}_{11} = \tilde{Q}_{11}$, $\bar{R}_{22} = \tilde{R}_{22}$, $\bar{R}_{21} = \tilde{R}_{21}$, and $\bar{Q}_{21} = \tilde{Q}_{21}$. For $K_{21} = -P_{22}^{-1}P_{21}$ one has $\bar{Q}_{11} = Q_{11}$, $\bar{R}_{22} = P_{22}$, $\bar{R}_{21} = 0$, and $\bar{Q}_{21} = Q_{21}$.

REFERENCES

1. Tischler, M. B., Berger, T., Ivler, C. M., Mansur, M. H., Cheung, K. K., and Soong, J. Y., *Practical Methods for Aircraft and Rotorcraft Flight Control Design: An Optimization-Based Approach*, AIAA Education Series, Reston, VA, 2017.

2. McRuer, D., Ashkenas, I., and Graham, D., *Aircraft Dynamics and Automatic Control*, Princeton University Press, Princeton, New Jersey, 1973. DOI: 10.1515/9781400855988.

3. Ivler, C. M., "Constrained State-Space Coupling Numerator Solution and Helicopter External Load Control Design Application," *Journal of Guidance, Control, and Dynamics*, Vol. 38, (10), October 2015, pp. 2004–2010. DOI: 10.2514/1.G001093.

4. Catapang, D. R., Tischler, M. B., and Biezad, D. J., "Robust crossfeed design for hovering rotorcraft," *International Journal of Robust and Nonlinear Control*, Vol. 4, (1), 1994, pp. 161–180. DOI: 10.1002/rnc.4590040110.

5. Hess, R. A., "Coupling Numerators and Input-Output Pairing in Square Control Systems," *Journal of Guidance, Control, and Dynamics*, Vol. 26, (2), March 2003, pp. 367–369. DOI: 10.2514/2.5056.

6. Celi, R., "Numerical Calculation of High-order, Constrained Inner Loop Transfer Functions," 30th European Rotorcraft Forum, Marseilles, France, 2004.

7. Moness, M., and Amin, M. H., "Minimal-order precompensators for decoupling linear multivariable systems S(A, B, C, E)," *International Journal of Control*, Vol. 47, (6), June 1988, pp. 1925–1936. DOI: 10.1080/00207178808906147.

8. Skogestad, S., "Advanced Control Using Decomposition and Simple Elements," *Annual Reviews in Control*, Vol. 56, January 2023, pp. 1–44. DOI: 10.1016/j.arcontrol.2023.100903.

9. Seher-Weiß, S., "ACT/FHS System Identification Including Rotor and Engine Dynamics," *Journal of the American Helicopter Society*, Vol. 64, (2), April 2019, pp. 1–12. DOI: 10.4050/JAHS.64.022003.